The X-Ray-Faint Early-Type Galaxy NGC 4697

Jimmy A. Irwin – University of Michigan
Craig L. Sarazin – University of Virginia
Joel N. Bregman – University of Michigan

Citation of published version:

Irwin, J., Sarazin, C., Bregman, J. (2000): The X-Ray-Faint Early-Type Galaxy NGC 4697. *The Astrophysical Journal Letters*, 544(2). DOI: 10.1086/317196

THE ASTROPHYSICAL JOURNAL, 544:293–301, 2000 November 20

THE X-RAY–FAINT EARLY-TYPE GALAXY NGC 4697

JIMMY A. IRWIN,[1,2] CRAIG L. SARAZIN,[3] AND JOEL N. BREGMAN[1]
Received 2000 March 7; accepted 2000 June 27

ABSTRACT

We analyze archival *ROSAT* HRI, *ROSAT* PSPC, and *ASCA* data of the X-ray–faint early-type galaxy NGC 4697. The joint *ROSAT* PSPC+*ASCA* spectrum is fitted by a two-component thermal model, a MEKAL model with $kT_{\rm MEKAL} = 0.26^{+0.04}_{-0.03}$ keV with low metallicity and a bremsstrahlung model with $kT_{\rm BREM} = 5.2^{+3.0}_{-1.6}$ keV. A similar model was found to fit the spectra of another faint early-type galaxy (NGC 4382) and the bulge of M31. We interpret this soft emission as a combination of emission from a soft component of low-mass X-ray binaries (LMXBs) and from a low-temperature interstellar medium, although the relative contributions of the two components could not be determined. Twelve point sources were identified within 4′ of NGC 4697, of which 11 are most likely LMXBs associated with the galaxy. The soft X-ray colors of four of the LMXBs in NGC 4697 support the claim that LMXBs possess a soft spectral component. Finally, we present a simulation of what we believe the *Chandra* data of NGC 4697 will look like.

Subject headings: binaries: close — galaxies: elliptical and lenticular, cD — galaxies: ISM — X-rays: galaxies — X-rays: ISM — X-rays: stars

1. INTRODUCTION

It is well established that early-type galaxies exhibit a large range of X-ray–to–optical luminosity ratios, L_X/L_B. Although there is a strong correlation between the X-ray and optical luminosities of elliptical and S0 galaxies ($L_X \propto L_B^{1.7}-L_B^{3.0}$; Canizares, Fabbiano, & Trinchieri 1987; White & Davis 1997; Brown & Bregman 1998), a large dispersion exists in this relation. Two galaxies with similar blue luminosities might have X-ray luminosities that differ by as much as a factor of 100 (Canizares et al. 1987; Fabbiano, Kim, & Trinchieri 1992; Brown & Bregman 1998).

Hot ($\sim 10^7$ K) gas is believed to be responsible for the bulk of the X-ray emission in high-L_X/L_B galaxies (e.g., Forman, Jones, & Tucker 1985). Another possible source of X-ray emission in early-type galaxies is from discrete stellar sources, primarily low-mass X-ray binaries (LMXBs). Estimates for the stellar L_X/L_B value are uncertain and vary by a factor of 10 among various studies (Forman et al. 1985; Canizares et al. 1987). Although stellar X-ray sources are not expected to contribute significantly to the 0.1–2.0 keV X-ray emission in gas-rich, X-ray–bright galaxies, this claim cannot be made with any certainty for X-ray-faint (low L_X/L_B) galaxies. In these galaxies it is possible that stellar X-ray sources are the dominant X-ray emission mechanism. For this to occur, the gas lost from stellar mass loss must be removed from the galaxy by galactic winds, by ram pressure stripping from ambient intracluster or intragroup gas, or possibly both (see, e.g., Ciotti et al. 1991; Mathews & Brighenti 1998).

Evidence is mounting that LMXB emission is detectable in nearly all early-type galaxies. Matsumoto et al. (1997) found a hard ($\sim$5–10 keV) spectral component in 11 of 12 early-type galaxies observed with *ASCA*, which scaled roughly with the optical luminosity of the galaxy (note, however, that Buote & Fabian 1998 found no formal need for a hard component in the X-ray–brightest galaxies of their *ASCA* sample). The luminosity of this hard component was small compared to the soft, gaseous component in the X-ray–brightest galaxies but increased in importance as L_X/L_B decreased. However, the *ASCA* observations did not resolve this component into discrete sources because of the insufficient spatial resolution of the instrument.

Previous studies have found that the spectra of the X-ray–faintest early-type galaxies are significantly different than the spectra of gas-rich X-ray–bright early-type galaxies. *Einstein* data revealed that the X-ray–faintest galaxies exhibited a strong very soft X-ray excess (Kim, Fabbiano, & Trinchieri 1992). Subsequent *ROSAT* PSPC and *ASCA* studies found that the spectra of these galaxies were best fitted with a two-component model consisting of the previously mentioned hard $\sim$5–10 keV component (generally attributed to the integrated LMXB emission) and a very soft $\sim$0.3 keV component whose origin is uncertain (Fabbiano, Kim, & Trinchieri 1994; Pellegrini 1994; Kim et al. 1996).

One recently proposed solution to the very soft X-ray excess problem in X-ray–faint galaxies is that it might result from the very same collection of LMXBs responsible for the hard emission (Irwin & Sarazin 1998a, 1998b). Little is known about the very soft X-ray properties of LMXBs since nearly all Galactic examples lie in directions of high Galactic hydrogen column densities, so their soft X-ray emission is heavily absorbed. However, two nearby Galactic LMXBs that lie in directions of low Galactic hydrogen column density (Her X-1 and MS 1603+2600) exhibit significant very soft X-ray emission (Vrtilek et al. 1994; Hakala et al. 1998). But perhaps the strongest evidence comes from the bulge of M31. M31 is close enough that most ($\gtrsim$75%) of its bulge X-ray emission was resolved into point sources with the *ROSAT* PSPC and HRI (Primini, Forman, & Jones 1993; Supper et al. 1997), a majority of which are probably LMXBs. Both individually and cumulatively, these point sources in the bulge of M31 have X-ray spectral properties very similar to the integrated emission from X-ray–faint

[1] Department of Astronomy, University of Michigan at Ann Arbor, 501 East University Avenue, Ann Arbor, MI 48109-1090; jirwin@astro.lsa.umich.edu, jbregman@umich.edu.
[2] Chandra Fellow.
[3] Department of Astronomy, University of Virginia, P.O. Box 3818, Charlottesville, VA 22903-0818; cls7i@virginia.edu.

early-type galaxies in the *ROSAT* band (Irwin & Sarazin 1998a, 1998b). A joint *ROSAT* PSPC + *ASCA* study found the X-ray spectrum of the bulge of M31 to be almost identical to that of the X-ray–faint early-type galaxy NGC 4382 over the 0.2–10 keV band (Kim et al. 1996; Irwin & Bregman 1999b). The bulge of the Sa galaxy NGC 1291 also exhibits a very soft component and has X-ray colors identical to the bulge of M31, although it is unresolved with *ROSAT* because of its distance. In both bulges, the measured L_X/L_B value is comparable to those of the X-ray–faintest early-type galaxies. This suggests that in addition to providing the required spectral X-ray characteristics, LMXBs are luminous and/or numerous enough to produce the required amount of X-ray emission in the X-ray–faintest early-type galaxies as well as Sa spiral bulges. No additional very soft X-ray emission source seems to be required.

In this paper we analyze long *ROSAT* PSPC, *ROSAT* HRI, and *ASCA* GIS and SIS observations of the X-ray–faint elliptical galaxy NGC 4697. At a distance of 15.9 Mpc (Faber et al. 1989; assuming a Hubble constant of 50 km s^{-1} Mpc^{-1}), NGC 4697 is one of the closest normal early-type galaxies. Previous work has indicated that this galaxy has a below average but not extremely low L_X/L_B value and *ROSAT* band colors typical of those of other X-ray–faint early-type galaxies (Irwin & Sarazin 1998b). Jointly fitting the *ROSAT* PSPC and *ASCA* spectra allows us to place useful constraints on both the hard and soft emission, something that is not possible using each instrument separately. In addition, NGC 4697 was one of the very few X-ray–faint early-type galaxies observed at length with the *ROSAT* HRI. We analyze this HRI image of NGC 4697 to resolve as much of the X-ray emission as possible into discrete sources. We also present a *Chandra* simulation of what the X-ray emission of NGC 4697 might look like.

2. *ROSAT* PSPC AND *ASCA* DATA REDUCTION

From the HEASARC archive we have extracted long *ROSAT* PSPC (rp600262a02) and *ASCA* GIS and SIS (62014000) observations of NGC 4697. The PSPC data were filtered such that all data with a master veto rate below 170 counts s^{-1} were excluded from the data, yielding an observation time of 36,856 s. The *ASCA* data were screened using the standard screening criteria applied to all the archival data (revision 2 processing). See Makishima et al. (1996) and Ohashi et al. (1996) for a description of the *ASCA* instruments. The total GIS and SIS exposure times were 56,698 and 42,138 s, respectively. The SIS observation was taken in 2-CCD mode.

Spectra from a 4′ radius were extracted from the PSPC, GIS, and SIS data. An extraction area of this size provided a good compromise between the minimum suggested extraction region for SIS data and achieving a reasonable signal-to-noise ratio for the PSPC data. For the PSPC, we have chosen background from a source-free annular region 30′–40′ in extent corrected for vignetting. For the *ASCA* data, background was extracted from the deep blank sky data provided by the *ASCA* Guest Observer Facility. We used the same region filter to extract the background as we did the data so that both background and data were affected by the detector response in the same manner.

For the PSPC data, only energy channels between 0.2 and 2.0 keV were included in the fits, and for the *ASCA* data we used energy channels between 0.8 and 10 keV. The energy channels were regrouped so that each channel contained at least 25 counts so that the χ^2 test is a valid indicator of goodness of fit. For all the joint fits, we linked the normalizations of the PSPC and GIS but let the SIS normalization vary to account for the fact that some of the emission that fell on interchip boundaries of the SIS was lost.

3. SPECTRAL MODELING AND LUMINOSITIES OF THE GLOBAL SPECTRUM

Using XSPEC Version 10.0, we first attempted to fit a single-component thermal model to the PSPC and *ASCA* data separately. When the PSPC spectrum was fitted alone with a MEKAL model with a variable absorption component a good fit was obtained ($\chi^2_\nu = 1.07/58$ degrees of freedom) for $kT = 0.43$–0.56 keV and $Z < 0.02$ (90% confidence level), in good agreement with the analysis of the same data by Davis & White (1996). A significantly different result was found for this same model when just the *ASCA* spectra were analyzed; the best-fit values were $kT = 2.2$–3.9 keV and $Z < 0.20$, with $\chi^2_\nu = 1.44/53$ degrees of freedom. Clearly, significantly different conclusions would be drawn from the spectra if data from only one of the satellites were analyzed.

This result illustrates the necessity of using both *ROSAT* PSPC and *ASCA* data when analyzing the spectrum of X-ray–faint early-type galaxies. When a one-component MEKAL model with a variable absorption component was fitted to the joint PSPC + *ASCA* spectrum, a poor fit was obtained ($\chi^2_\nu = 2.08/115$ degrees of freedom), with $kT = 0.82$ keV and $Z < 0.006$. Following the work of Kim et al. (1996) and Irwin & Bregman (1999b), we added a bremsstrahlung model in the fit. The MEKAL + bremsstrahlung model provided an excellent fit to the data ($\chi^2_\nu = 0.94/113$ degrees of freedom), with the absorption value fixed at the Galactic line-of-sight value of 2.12×10^{20} cm^{-2} (Stark et al. 1992). The MEKAL model had parameter values of $kT_{\rm MEKAL} = 0.26^{+0.04}_{-0.03}$ keV and $Z = 0.07^{+0.05}_{-0.03}$ (all errors are 90% confidence levels for one interesting parameter). The best-fit bremsstrahlung temperature was $kT_{\rm BREM} = 5.2^{+3.0}_{-1.6}$ keV. Freeing the absorption parameter led to only a slight improvement in the fit, and the 90% confidence value on $N_{\rm H}$ was consistent with the Galactic value.

We hesitate to attach a physical significance to this MEKAL + bremsstrahlung model. The spectra of individual Galactic LMXBs are often fitted by a disk-blackbody + blackbody (DBB + BB) spectrum (see, e.g., Mitsuda et al. 1984). The MEKAL + bremsstrahlung model, however, provided a good fit to the X-ray–faint early-type galaxy NGC 4382 (Kim et al. 1996) and the bulge of M31 (Irwin & Bregman 1999a; Trinchieri et al. 1999 showed that a Raymond-Smith + bremsstrahlung model adequately fitted the *BeppoSAX* LECS spectrum of the bulge of M31), whereas the DBB + BB model did not provide a good fit to the *ROSAT* PSPC + *ASCA* spectrum of the bulge of M31. Since we are interested in describing the spectrum of the a collection of LMXBs in the context of an elliptical galaxy and not of LMXBs on an individual basis, we will continue to use a MEKAL + bremsstrahlung model as has been done in previous studies of X-ray emission from early-type systems. We do not attempt to justify the physical relevance of the MEKAL + bremsstrahlung model, but use it here to quantify the strength of the soft and hard components of the X-ray emission.

Assuming a distance of 15.9 Mpc, the 0.25–10 keV luminosities of the soft and hard components were 1.50×10^{40} and 1.83×10^{40} ergs s^{-1}, respectively, in the 0.25–10 keV band. In the *ROSAT* band (0.1–2.4 keV) the luminosities were 2.36×10^{40} and 1.04×10^{40} ergs s^{-1}, respectively.

4. *ROSAT* HRI OBSERVATION OF NGC 4697

NGC 4697 was one of the few X-ray–faint early-type galaxies for which a long *ROSAT* HRI observation (rh600825a01) exists in the HEASARC archive (78,744 s). The observation did not contain any time intervals with excessively high background, so the entire observation was used. The inner $8' \times 8'$ of the HRI image is shown in Figure 1. A contour map of the HRI image is shown overlaying the Digital Sky Survey optical image in Figure 2. Several X-ray point sources are evident from the contour plot. Background-subtracted count rates were calculated for each point source detected within the same 4′ circle used to derive the PSPC and *ASCA* spectra. Background was selected from an annular ring with an inner and outer radii of 4′ and 6′ and was corrected for vignetting before being subtracted from the source. In all, 12 point sources were detected at a significance of 2 σ or higher, corresponding to a detection flux limit of 1.0×10^{-14} ergs s^{-1} cm^{-2} and a limiting luminosity of 3.0×10^{38} ergs s^{-1}. From the source counts catalog of a deep HRI observation by Hasinger et al. (1998), we would expect there to be ≤ 1 serendipitous source in a 4′ circle field at this flux level or higher. Thus, it is likely that all or nearly all of the X-ray sources in the field belong to NGC 4697.

The positions, number of counts, significance of detection, and luminosities of the 12 point sources are shown in Table 1. The count rates were converted to luminosities using the two-component spectral model found in § 3. Two of the sources (sources 6 and 11) are coincident within the position errors with faint optical point sources with magnitudes of approximately 18, which do not correspond to any QSO found in the Véron-Cetty & Véron (1998) catalog. The optical source near source 11 has been identified as a bright globular cluster of NGC 4697 (Hanes 1977). The central source in Figures 1 and 2 appears elongated in the north-south direction. When the center is viewed at higher resolution, the source is split into two sources (sources 7 and 8 in Table 1), which are separated by $\sim 7''$, close to the resolution limit of the HRI. Source 7 is within 2″ of the optical center of NGC 4697 (R.A. = $12^h48^m35^s.71$ and decl. = $-5°48'02''.9$), as given by Wegner et al. (1996). Given

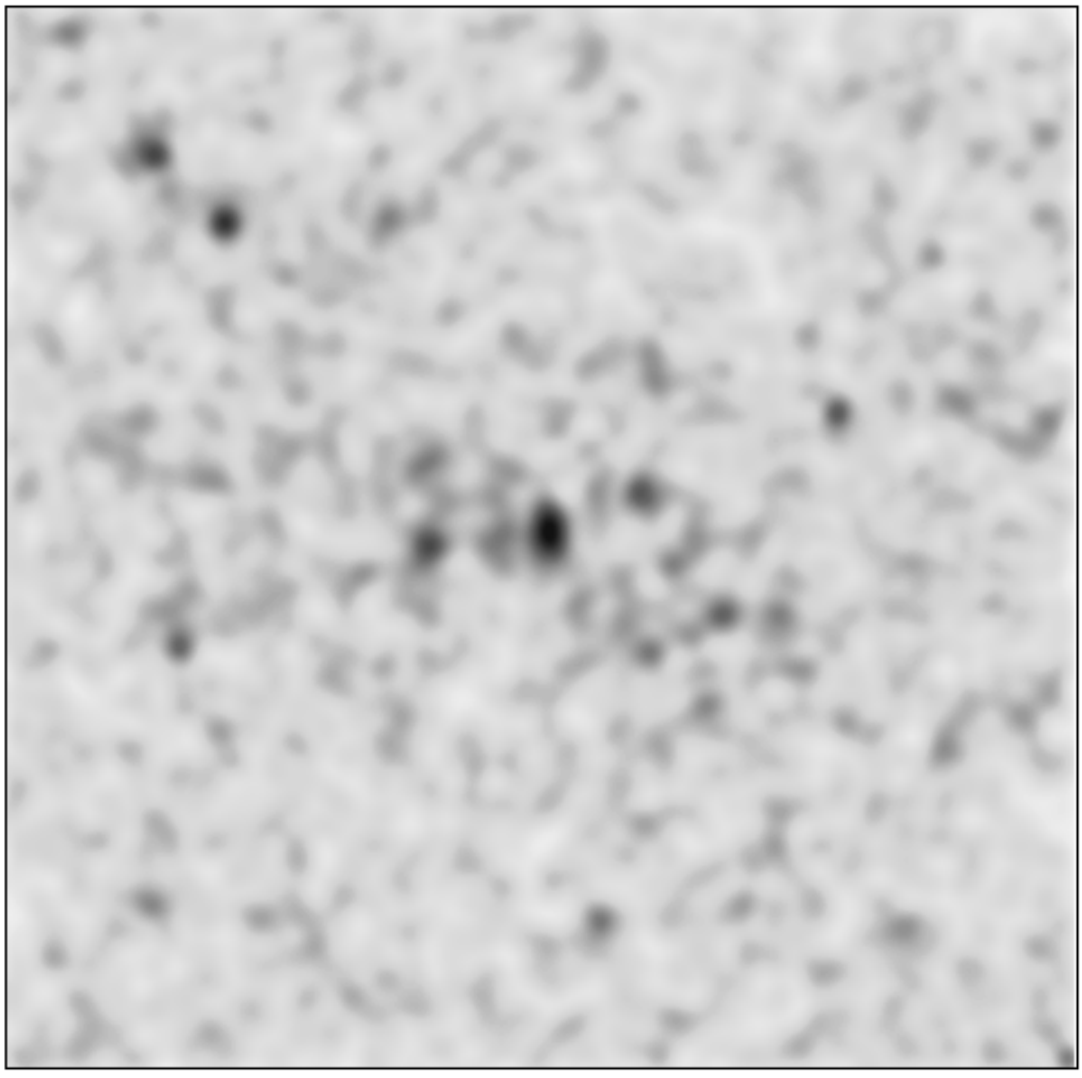

FIG. 1.—Inner $8' \times 8'$ of the *ROSAT* HRI image of NGC 4697. The HRI map has been smoothed with a Gaussian of 5″.

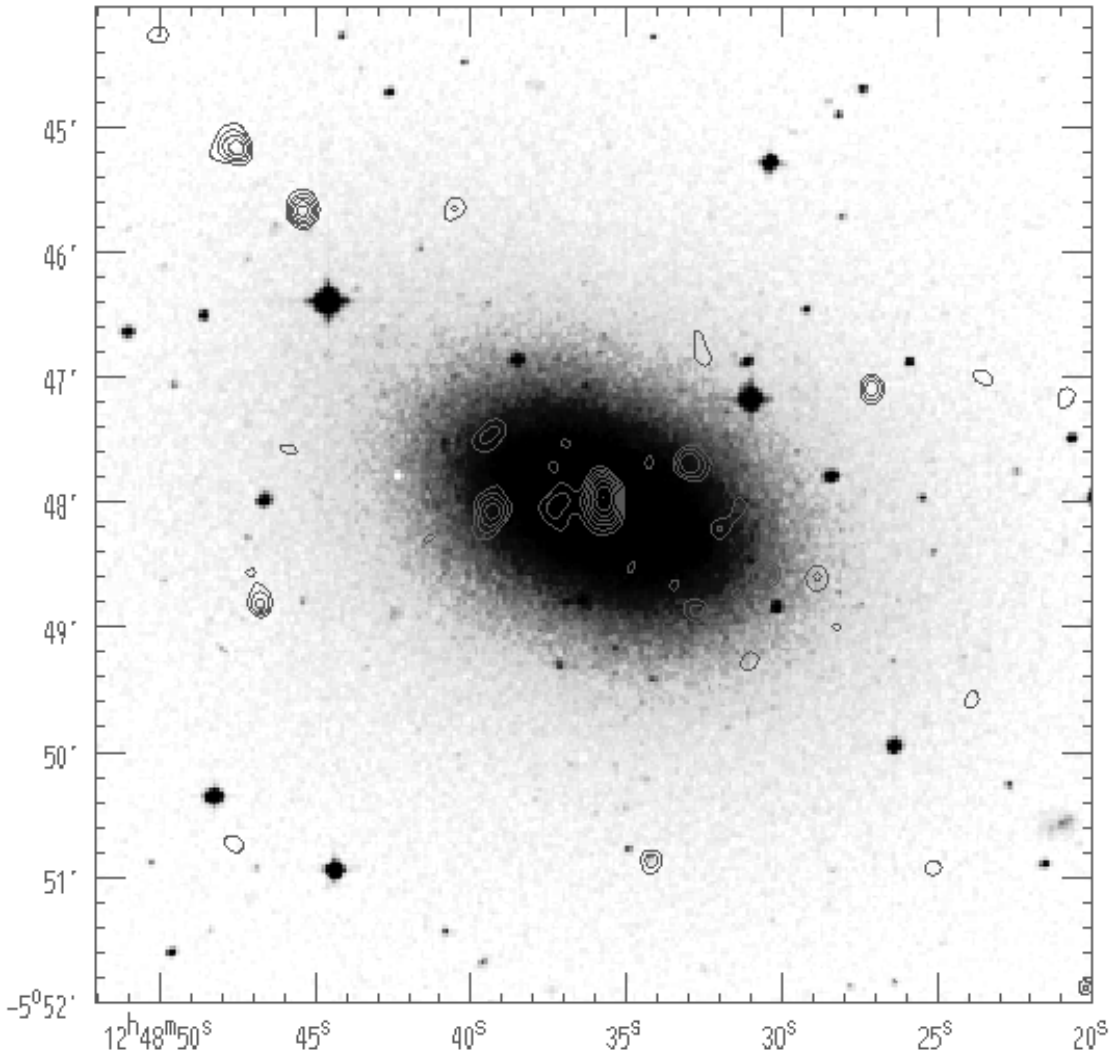

FIG. 2.—*ROSAT* HRI contour map overlaid the Digital Sky Survey image of NGC 4697. The HRI map has been smoothed with a Gaussian of 5″, and the contours have been chosen to highlight the point sources.

the HRI positional uncertainty of ∼5″, the additional uncertainty due to the crowding of sources 7 and 8 (which might contain additional components), and the optical position uncertainty of about 1.′25, it is possible that source 7 or even 8 might be coincident with the optical center of the galaxy. Thus, one of these sources might be due to an active nucleus in the galaxy. On the other hand, there is no evidence for an active galactic nucleus (AGN) in NGC 4697;

TABLE 1

HRI X-RAY SOURCES WITHIN 4′

Source	R.A.	Decl.	Counts	S/N	X-Ray Luminosity (ergs s^{-1})
1	12 48 27.13	−5 47 05.3	27.6 ± 7.4	3.7	7.0×10^{38}
2	12 48 30.54	−5 48 34.3	17.6 ± 6.5	2.7	4.4×10^{38}
3	12 48 32.05	−5 48 14.1	14.1 ± 6.20	2.3	3.6×10^{38}
4	12 48 32.60	−5 48 52.3	16.2 ± 6.4	2.5	4.1×10^{38}
5	12 48 33.03	−5 47 39.8	22.1 ± 6.9	3.2	5.6×10^{38}
6	12 48 34.24	−5 50 51.5	17.8 ± 6.5	2.7	4.5×10^{38}
7[a]	12 48 35.65	−5 48 01.3	30.5 ± 11.3	2.7	7.7×10^{38}
8[a]	12 48 35.68	−5 47 54.3	30.0 ± 11.3	2.7	7.6×10^{38}
9	12 48 39.30	−5 48 03.9	20.0 ± 6.7	3.0	5.0×10^{38}
10.....	12 48 45.41	−5 45 40.1	32.8 ± 7.8	3.5	8.3×10^{38}
11.....	12 48 46.77	−5 48 51.1	17.8 ± 6.5	4.2	4.5×10^{38}
12.....	12 48 47.42	−5 45 10.0	24.0 ± 7.1	3.4	6.0×10^{38}

NOTE.—Units of right ascension are hours, minutes, and seconds, and units of declination are degrees, arcminutes, and arcseconds.

[a] Count rate and luminosity are uncertain because of crowding.

for example, the nucleus is not a radio source (e.g., the NRAO VLA Sky Survey; Condon et al. 1998). The positive detection of only 12 sources does not allow us to determine if the sources follow the de Vaucouleurs stellar distribution, especially considering that one if not more of the sources is associated with a globular cluster of NGC 4697 and crowding in the center will underestimate the number of detected point sources in this region.

What is not evident from Figure 2 is the presence of very faint unresolved X-ray emission within 4′ (the contours of Fig. 2 were chosen to highlight the position of the X-ray point sources). Figure 3 shows the contours from a more heavily smoothed HRI image once again overlaying the optical image. The emission appears elongated in the direction of the optical major axis of the galaxy. The surface brightness profile of the X-ray emission follows the optical surface brightness profile derived by Jedrzejewski, Davies, & Illingworth (1987) out to 4′, suggesting that the X-ray emission is distributed like the stars. However, it was found that a β-model profile with a shallow slope ($\beta = 0.4$–0.45) also fitted the data adequately. The faint unresolved emission is actually the dominant source of emission in the HRI image, comprising 79% of the total emission. The nature of this unresolved emission is discussed next.

5. DISCUSSION

The 12 point sources detected within 4′ of NGC 4697 constitute 21% of the total X-ray emission of the galaxy. The question remains as to whether the remaining unresolved emission is the summed emission from LMXBs below the detection threshold of the HRI or is a low-temperature interstellar medium (ISM) with $kT \sim 0.25$ keV. The absorbed flux of the hard component found from the spectral fitting of the PSPC and *ASCA* data sets a lower limit on the contribution of LMXBs to the unresolved emission. In the *ROSAT* band the hard component contributes 40% of the total (unabsorbed) flux. Thus, even if LMXBs possess only a hard X-ray component, another $\sim$20% of the total emission must result from LMXBs below the detection threshold of the HRI.

As mentioned in the introduction, LMXBs might also possess a soft X-ray component. This component would have gone unnoticed in most Galactic disk or bulge LMXBs, where the high Galactic column densities associated with the Galactic plane would completely absorb any very soft emission. Although there does not appear to be a soft component toward Galactic globular cluster LMXBs that lie in directions of low column densities, this might be

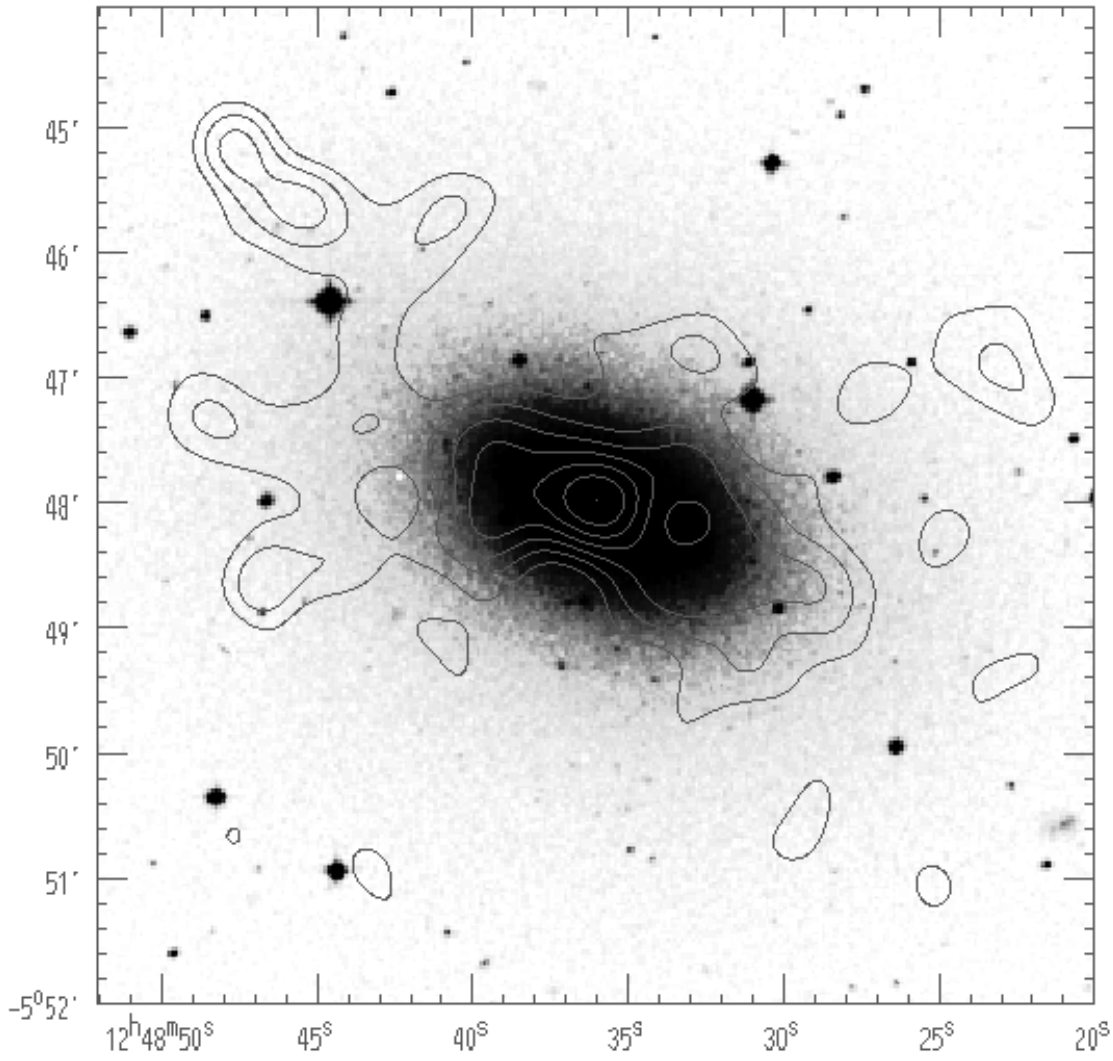

FIG. 3.—*ROSAT* HRI contour map overlaid the Digital Sky Survey image of NGC 4697. The HRI map has been smoothed with a Gaussian of 15″, and the contours have been chosen to highlight the unresolved emission.

the effect of the low metallicities in which the LMXBs formed (see Irwin & Bregman 1999a). The bulge of M31, however, provides the nearest opportunity to study a sample of LMXBs in an environment most similar to that found in early-type galaxies. Supper et al. (1997) analyzed the *ROSAT* PSPC image of M31 and found 22 point sources within the inner 5′ of the bulge with luminosities in the range 10^{36}–10^{38} ergs s^{-1}. Individually, these point sources had X-ray colors that indicated the presence of a significant soft component. Seven of the 22 sources had enough counts for Supper et al. (1997) to perform spectral fitting. The best-fit bremsstrahlung temperatures ranged from 0.45 to 1.5 keV, very similar to the result found for NGC 4697 for the same model. Although such a simplistic model is not physically plausible, it did indicate that the spectrum of the LMXBs were significantly softer than the canonical temperature of 5–10 keV previously assumed for LMXBs.

We can search for such a soft component in the point sources suspected to be LMXBs in NGC 4697. Of the 12 point sources detected by the HRI, sources 1, 6, 10, 11, and 12 were also detected and resolved in the PSPC (sources 10 and 12 were marginally resolved from each other in the PSPC). As mentioned above, source 6 might be associated with background/foreground objects. The counts from the other four sources were summed in three energy bands, and two X-ray colors (C21 and C32) were defined from the ratio of the three bands:

$$\mathrm{C21} = \frac{\text{counts in PI bins 52–90}}{\text{counts in PI bins 11–41}}, \quad (1)$$

$$\mathrm{C32} = \frac{\text{counts in PI bins 91–202}}{\text{counts in PI bins 52–90}}. \quad (2)$$

Note that these colors are not corrected for absorption.

Sources 1, 10, 11, and 12 combined yielded 359.5 background-subtracted counts, or 14% of the total X-ray emission within 4′ in the PSPC image. The colors for the sources were (C21, C32 = 0.57 ± 0.09,0.94 ± 0.16). As a comparison, the colors for all emission within 4′ were (C21, C32 = 0.68 ± 0.05,0.77 ± 0.05). Thus, the colors of the four resolved sources are consistent with the colors for the integrated emission from the galaxy. This argues that the four LMXBs must also possess a soft component similar to that found in the global spectrum. Otherwise, the integrated emission would have had significantly different colors than the point sources. Conversely, the colors predicted from a 5.2 keV bremsstrahlung model with an absorbing column density of 2.12×10^{20} cm^{-2} were (C21, C32 = 1.204,1.893). This differs from the colors of the four point sources by 7.0 σ and 6.0 σ for C21 and C32, respectively. Clearly, if LMXBs were described by only a hard component, the colors of the four point sources would be significantly harder than what they are.

We have calculated the colors of NGC 4697 in elliptical annuli (with ellipticity of 0.42 and a position angle of 67° to match the optical profile; Fig. 4). C32 peaks inside of 1.′5 but flattens at larger radii, while C21 is constant throughout the galaxy. The peak in C32 may result from the presence of an AGN in NGC 4697. The constancy of C21 and C32 outside of 1.′5 implies a single emission mechanism (or two emission mechanisms with the same spatial distribution) with colors around 0.6 for both colors, in rough agreement with the colors of the four point sources. The C32 color of the diffuse emission is somewhat lower than the C32 value of the four point sources, possibly indicating the presence of an ISM component, although the discrepancy between the two colors is only at the 2 σ level. The colors predicted from a 0.2 keV, 20% metallicity ISM are (C21, C32 = 0.54, 0.22), whereas the colors for a 0.3 keV, 20% metallicity ISM are (C21, C32 = 1.17, 0.46). Thus, if any ISM is present in NGC 4697, its temperature must be below 0.3 keV and at a low metallicity or else the C21 color of the LMXBs+ISM would be higher than the LMXBs alone, which is not observed. In conclusion, we cannot rule out the presence of some low-temperature ISM in NGC 4697, although it is certain that an ISM cannot constitute a majority of the emission.

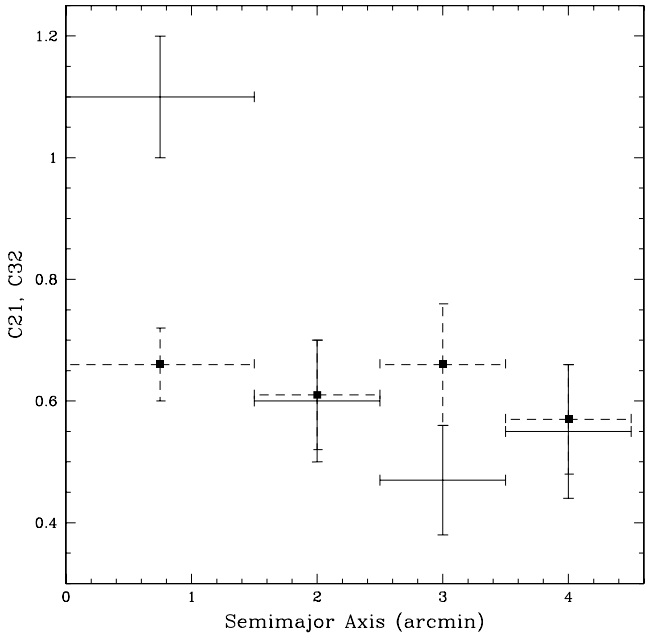

FIG. 4.—C21 (*dotted lines*) and C32 (*solid lines*) colors derived from the PSPC data as a function of semimajor axis for NGC 4697.

Irwin & Bregman (1999a) found that Galactic and M31 globular cluster LMXB X-ray colors were correlated with the metallicity of the globular cluster, in the sense that higher metallicity globular clusters had LMXBs with softer X-ray colors. If this correlation extended to all LMXBs, it would predict that the X-ray colors of NGC 4697 should harden with increasing radius, since metallicity decreases with radius in elliptical galaxies. Furthermore, the metallicity of NGC 4697 is rather low. Within half an effective radius the average metallicity is only 50% solar (Trager et al. 2000). The metallicity-color relation of Irwin & Bregman (1999a) would predict a C32 color of about 1.5 within half an effective radius and an increase with increasing radius. The colors of the four resolved sources as well as the unresolved emission are at odds with this metallicity-color relation. Apparently, if such a metallicity-color relation truly exists for LMXBs, it only applies to LMXBs that reside in globular clusters. The X-ray source in NGC 4697 associated with a globular cluster (source 11) has a C32 color of 1.14 ± 0.30, which would be consistent with the metallicity-color relation if the globular cluster has a high metallicity.

We also investigated the possibility that LMXBs below the detection threshold of the HRI could account for the

unresolved emission given a reasonable LMXB luminosity distribution function for NGC 4697. We assumed a luminosity distribution function $N(>L_X) \propto L_X^{-1.3}$, which is consistent within the errors with the luminosity distribution function of point sources in M31 with luminosities greater than 2×10^{37} ergs s^{-1} (Primini et al. 1993). The function was normalized to yield the observed X-ray luminosity of NGC 4697 when integrated over all LMXB luminosities. This model predicted 11 sources with luminosities over 3×10^{38} ergs s^{-1}, which contributed 18% to the total X-ray emission from LMXBs. This agrees well with what was observed with the HRI; neglecting the point source associated with an unidentified optical counterpart, the remaining 11 detected sources comprised 19% of the total emission. Thus, if the luminosity distribution function of LMXBs of NGC 4697 is similar to that of the brighter LMXBs in M31, the integrated emission from LMXBs below the detection threshold of the HRI can account for most of the unresolved emission.

Interestingly, the detection limit of the HRI observation of 3×10^{38} ergs s^{-1} lies above the Eddington luminosity limit for a 1.4 $M_\odot$ neutron star. LMXBs of similar luminosities as the ones found here exist in our own Galaxy. A compilation by Christian & Swank (1997) found eight Galactic LMXBs with luminosities greater than 3×10^{38} ergs s^{-1} (we have converted their 0.7–4.5 keV luminosities to 0.25–10 keV luminosities using the spectral model of § 3). These high luminosities imply either that the compact object within the binary is a black hole (with $M_{BH} \geq 6\ M_\odot$ for the most luminous binaries) or that the luminosities truly exceed the Eddington limit for a neutron star. The former would imply that active binaries with massive black holes are fairly common in galaxies. It should be noted that the bulge of M31 lacks the very high luminosity LMXBs that NGC 4697 has; the brightest LMXB in M31 was only 1.8×10^{38} ergs s^{-1} (Supper et al. 1997). However, this is likely the result of small number statistics. Simulations of the bulge of M31 using a luminosity distribution function of the form $N(>L_X) \propto L_X^{-1.13}$ indicated that only one to three sources with luminosities exceeding 10^{38} ergs s^{-1} should be found in M31. In five separate simulations of M31 the peak luminosity for an LMXB did not exceed 3×10^{38} ergs s^{-1}, in agreement with observation.

We cannot rule out the presence of at least some ISM in NGC 4697 and X-ray–faint early-type galaxies in general. Using the X-ray temperature-optical velocity dispersion relation of Davis & White (1996), any ISM present in NGC 4697 would be expected to have a temperature around 0.3 keV. This would be very difficult to distinguish from the soft component from LMXBs on a spectroscopic basis alone. What is needed to separate the ISM component from the LMXB emission is the high spatial resolution that can be afforded by *Chandra*. Below we present a simulation of what we expect the emission from NGC 4697 to look like in the event that the emission is composed solely of LMXBs.

6. SIMULATION OF *CHANDRA* OBSERVATION OF NGC 4697

We have an approved Cycle 1 40,000 s *Chandra* observation of NGC 4697; here we show that this observation should resolve the hard and soft X-ray emission into individual sources, assuming that the emission is from LMXBs. Conversely, the observation should cleanly separate a truly diffuse emission from that of LMXBs. Since the main goal is to resolve the issue of the very soft component, the soft X-ray sensitive backside-illuminated (BI) S3 chip of the ACIS-S array will be used for the observation. We have used the MARX (Model of *AXAF* Response to X-rays; Wise, Huenemoerder, & Davis 1997) Simulator to generate a synthetic image of NGC 4697. The MARX Simulator takes as input the desired spectral model and spatial distribution model of an X-ray source and creates an image of the source as it would appear once having passed through the optics of *Chandra*. The spectral and spatial distribution models described below were fed into MARX using the ACIS-S BI response to produce an image of NGC 4697 for a 40,000 s observation.

For the spectra of the LMXBs, we assume a model that best fitted the joint *ROSAT* PSPC+*ASCA* spectrum of NGC 4697 discussed in § 3. For the spatial distribution of the X-ray emission, we assume that the LMXBs have the same spatial distribution as the stellar light. We take the optical distribution to be a de Vaucouleurs profile (de Vaucouleurs et al. 1991) with a mean half-light radius of 72″, an effective semimajor axis of 95″, and an effective semiminor axis of 55″, resulting in an ellipticity of 0.42 and elongated at a position angle of 67°. (Jedrzejewski et al. 1987; Faber et al. 1989; Peletier et al. 1990). As before, we assume a luminosity distribution function for the LMXBs of the form $N(>L_X) \propto L_X^{-1.3}$. The luminosity distribution function contained point sources with 0.25–10.0 keV luminosities between 10^{37} and 10^{39} ergs s^{-1}. A model galaxy was created by drawing LMXBs at random from the luminosity distribution function and the spatial distribution until the sum of the luminosities of the LMXBs totaled the X-ray luminosity of the galaxy. We did not use the observed positions and fluxes of the sources in Table 1 in the model; the sources are randomly drawn from the optical surface brightness distribution and X-ray luminosity distribution. We did not include background in this simulation. The background in the *Chandra* ACIS S-3 chip is highly variable (Markevitch 1999[4]), and its level during the observation will affect the ability to detect the weakest sources.

Figure 5 shows the simulated image of NGC 4697. The image shows the inner 4′ × 4′ of the galaxy. The excellent spatial resolution of *Chandra* is evident. The dynamic range of the source brightness in this image is not clear from this grayscale representation, since all of the strong sources are nearly the same size (set by the resolution) and black. However, the sources cover a range of ~25 in flux. For our simulation, we assumed that 16 source counts would be needed to give a 3 σ detection considering the variable background of the ACIS S-3 chip. This assumption predicts that ~100 sources would be detected at $\geq 3\ \sigma$ with a detection threshold of 6×10^{37} ergs s^{-1}. These 100 sources comprise 50% of the total luminosity of the galaxy. In the 0.25–0.8 keV band, ~50 sources were detected at $\geq 3\ \sigma$.

We have also simulated a *Chandra* image where the LMXBs have only a hard (5.2 keV) bremsstrahlung component that comprises 59% of the 0.25–10 keV emission (this was the relative contribution of the hard component to the total emission found in § 3). In this case, only about 12 LMXBs were detected in the 0.25–0.8 keV band. If LMXBs do possess a soft component, it will be immediately obvious

[4] ACIS Background (Markevitch 1999) is available at http://asc.harvard.edu/cal/Links/Acis/acis/Cal_prods/bkgrnd/11_18/bg181199.html.

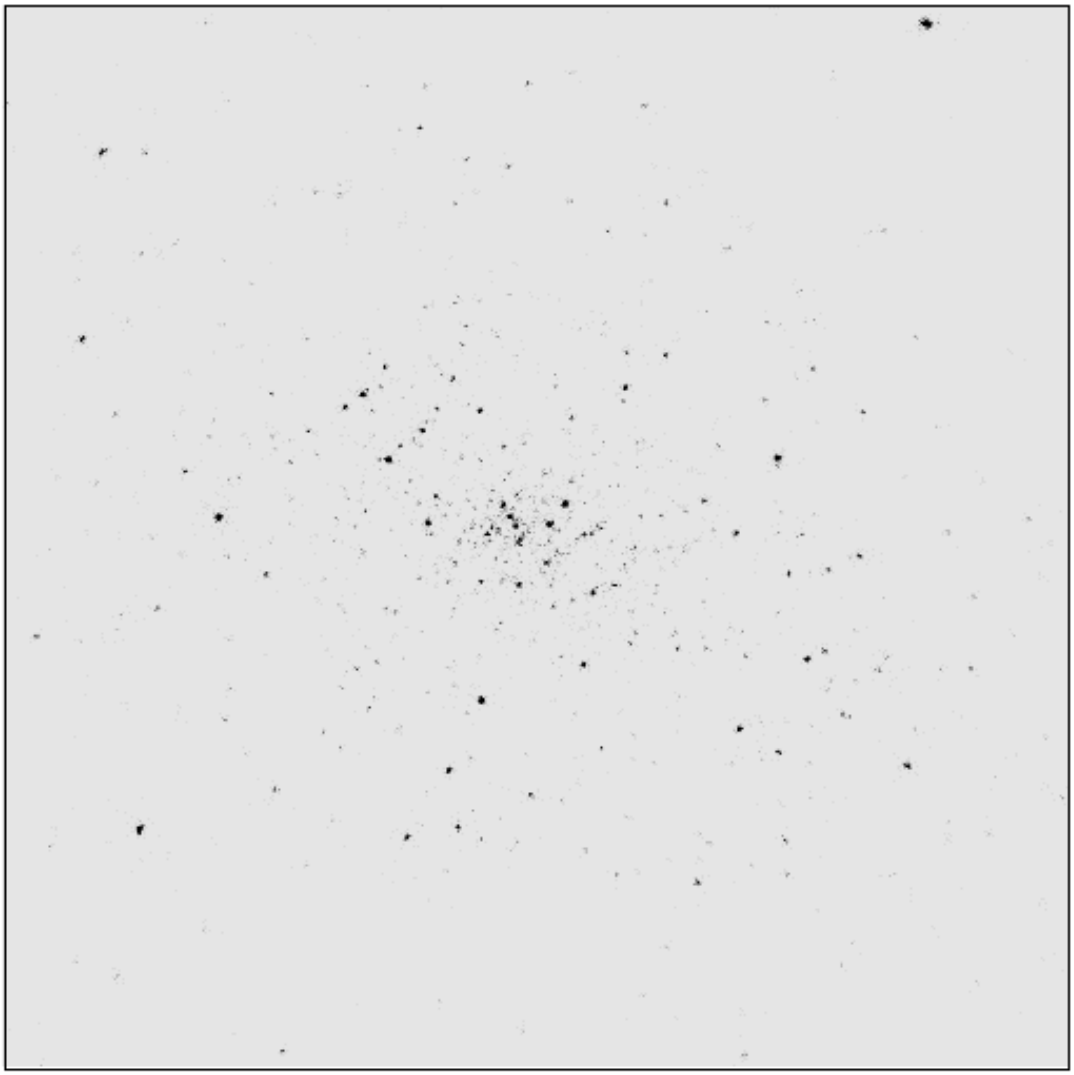

FIG. 5.—40,000 s *Chandra* simulation of the inner 4′ × 4′ of NGC 4697 in the 0.25–10 keV range, assuming all of the X-ray emission from NGC 4697 is from LMXBs.

from the 0.25–0.8 keV *Chandra* image of NGC 4697. X-ray spectra of some of the brighter sources, X-ray colors of fainter sources, the cumulative X-ray spectra of individual sources, and of any remaining unresolved diffuse emission can be determined and should resolve the question of the origin of the hard and soft X-ray components in X-ray–faint ellipticals.

A number of fundamental questions regarding the X-ray emission from early-type and Sa galaxies will be answered with *Chandra*. With the expected number of detectable LMXBs, accurate luminosity distribution functions can be determined. This is something that has been accomplished for only a handful of nearby galaxies, none of which are normal early-type galaxies. This will provide important clues to the stellar evolution of binary stars in galaxies. There is evidence that there may not be a universal stellar X-ray–to–optical luminosity ratio. A range of $L_{\rm X,stellar}/L_B$ values has been suggested by comparison of the X-ray emission of the bulge of M31 to that of Cen A (Turner et al. 1997) and also to several very X-ray–faint early-type galaxies in the Irwin & Sarazin (1998b) survey. If nearly all the X-ray emission in NGC 4697 turn out to be stellar in nature, it would be difficult to explain why the early-type galaxy NGC 5102, for example, has a 0.5–2.0 keV $L_{\rm X}/L_B$ value that is 19 times lower than that of NGC 4697 (Irwin & Sarazin 1998b), if $L_{\rm X}$, stellar/L_B is constant from galaxy to galaxy. Without knowledge of the luminosity distribution function, it cannot be determined if this difference is a result of a different slope in the distribution function among galaxies or if the slopes are the same but the normalizations of the function (relative to the optical luminosity of the galaxy) are different. The separation of the stellar and gaseous components is necessary to resolve this issue.

Since LMXB emission is expected to be present in all early-type galaxies, the magnitude of this component needs to be known accurately in order to subtract the LMXB contribution from the total X-ray emission in gas-rich early-type galaxies. This will make estimates of the mass of elliptical galaxies based on the assumption that the gas is in hydrostatic equilibrium more accurate. This is particularly important in the event that LMXBs possess a strong soft component. Although, the contribution of LMXBs to the total X-ray emission from very X-ray–bright Virgo elliptical galaxies such as NGC 4472 and NGC 4636 will be small

(less than 10% in the 0.1–2.4 keV band), LMXBs might contribute a significant percentage of the X-ray emission in galaxies of intermediate X-ray brightness and will have to be dealt with accordingly if the true amount of X-ray gas is to be determined.

7. CONCLUSIONS

We have analyzed deep *ASCA*, *ROSAT* PSPC, and *ROSAT* HRI images of the X-ray–faint early-type galaxy NGC 4697. Much like other X-ray–faint early-type systems, the spectrum of NGC 4697 is characterized by hard (5 keV) plus very soft (0.3 keV) emission. Whereas the nature of the hard emission is generally regarded as the integrated emission from LMXBs, we have provided additional evidence that much of the soft emission also emanates from LMXBs. Four of the 12 HRI point sources were resolved by the PSPC and were found to have soft X-ray colors that were very similar to those of the galaxy as a whole. These colors were significantly softer than the colors predicted if only the hard component was attributed to LMXBs.

The 12 point sources detected by the HRI comprised 21% of the total X-ray emission within 4′ of NGC 4697. Given a luminosity distribution function consistent with that for the brighter point sources in M31, the remaining unresolved emission could emanate solely from LMXBs below the detection threshold of the observation. However, the presence of a low-temperature ISM could not be completely ruled out. Higher spatial resolution data afforded by *Chandra* should successfully resolve much of the LMXB emission, as we have shown in our simulations. The determination of the origin of the soft component will have important implications concerning our understanding of the fate of gas lost from stars in galaxies as well as the X-ray emission mechanism of LMXBs.

We thank the referee, Fabrizio Brighenti, for many useful comments and suggestions concerning the manuscript. This research has made use of data obtained through the High Energy Astrophysics Science Archive Research Center Online Service, provided by the NASA/Goddard Space Flight Center. The optical image of NGC 4697 is from the Digital Sky Surveys, which were produced at the Space Telescope Science Institute. The images of these surveys are based on photographic data obtained using the Oschin Schmidt Telescope on Palomar Mountain and the UK Schmidt Telescope. J. A. I. was supported by *Chandra* Fellowship grant PF9-10009, awarded through the *Chandra* Science Center. The *Chandra* Science Center is operated by the Smithsonian Astrophysical Observatory for NASA under contract NAS 8-39073. C. L. S. was supported in part by NASA Chandra grant GO 0-1019X. J. N. B. was supported by NASA grant NAG 5-3247.

REFERENCES

Brown, B. A., & Bregman, J. N. 1998, ApJ, 495, L75
Buote, D. A., & Fabian, A. C. 1998, MNRAS, 296, 977
Canizares, C. R., Fabbiano, G., & Trinchieri, G. 1987, ApJ, 312, 503
Christian, D. J., & Swank, J. H. 1997, ApJS, 109, 177
Ciotti, L., Pellegrini, S., Renzini, A., & D'Ercole, A. 1991, ApJ, 376, 380
Condon, J. J., Cotton, W. D., Greisen, E. W., Yin, Q. F., Perley, R. A., Taylor, G. B., & Broderick, J. J. 1998, AJ, 115, 1693
Davis, D. S., & White, R. E., III 1996, ApJ, 470, L35
de Vaucouleurs, G. 1991, Third Reference Catalogue of Bright Galaxies (New York: Springer)
Fabbiano, G., Kim, D.-W., & Trinchieri, G. 1992, ApJS, 80, 531
———. 1994, ApJ, 429, 94
Faber, S. M., Wegner, G., Burstein, D., Davies, R. L., Dressler, A., Lynden-Bell, D., & Terlevich, R. J. 1989, ApJS, 69, 763
Forman, W., Jones, C., & Tucker, W. C. 1985, ApJ, 293, 102
Hakala, P. J., Chaytor, D. H., Vilhu, O., Piirola, V., Morris, S. L., & Muhli, P. 1998, A&A, 333, 540
Hanes, D. A. 1977, MmRAS, 84, 45
Hasinger, G., Burg, R., Giacconi, R., Schmidt, M., Trümper, J., & Zamorani, G. 1998, A&A, 329, 482
Irwin, J. A., & Bregman, J. N. 1999a, ApJ, 510, L21
———. 1999b, ApJ, 527, 125
Irwin, J. A., & Sarazin, C. L. 1998a, ApJ, 494, L33
———. 1998b, ApJ, 499, 650
Jedrzejewski, R. I., Davies, R. L., & Illingworth, G. D. 1987, AJ, 94, 1508
Kim, D.-W., Fabbiano, G., Matsumoto, H., Koyama, K., & Trinchieri, G. 1996, ApJ, 468, 175
Kim, D.-W., Fabbiano, G., & Trinchieri, G. 1992, ApJ, 393, 134
Makishima, K., et al. 1996, PASJ, 48, 171
Mathews, W. G., & Brighenti, B. 1998, ApJ, 503, L15
Matsumoto, H., Koyama, K., Awaki, H., Tsuru, T., Loewenstein, M., & Matsushita, K. 1997, ApJ, 482, 133
Mitsuda, K., et al. 1984, PASJ, 36, 741
Ohashi, T., et al. 1996, PASJ, 48, 157
Peletier, R. F., Davies, R. L., Illingworth, G. D., Davis, L. E., & Cawson, M. 1990, AJ, 100, 1091
Pellegrini, S. 1994, A&A, 292, 395
Primini, F. A., Forman, W., & Jones, C. 1993, ApJ, 410, 615
Stark, A. A., Gammie, C. F., Wilson, R. W., Bally, J., Linke, R. A., Heiles, C., & Hurwitz, M. 1992, ApJS, 79, 77
Supper, R., Hasinger, G., Pietsch, W., Trümper, J., Jain, A., Magnier, E. A., Lewin, W. H. G., & van Paradijs, J. 1997, A&A, 317, 328
Trager, S. C., Faber, S. M. Worthey, G., & González, J. J. 2000, AJ, 119, 1645
Trinchieri, G., Israel, G. L., Chiappetti, L., Belloni, T., Stella, L., Primini, F., Fabbiano, P., & Pietsch, W. 1999, A&A, 348, 43
Turner, T. J., George, I. M., Mushotzky, R. F., & Nandra, K. 1997, ApJ, 475, 118
Véron-Cetty, M. P., & Véron, P. 1998, ESO Sci. Rep. 18, A Catalogue of Quasars and Active Nuclei (8th ed.; Garching: ESO)
Vrtilek, S. D., et al. 1994, ApJ, 436, L9
Wegner, G., Colless, M., Baggby, G., Davies, R. L., Bertschinger, E., Burstein, D., McMahany, R. K., & Saglia, R. K. 1996, ApJS, 106, 1
White, R. E., III, & Davis, D. S. 1997, in Galactic and Cluster Cooling Flows, ed. N. Soker (San Francisco: ASP), 217
Wise, M. W., Huenemoerder, D. P., & Davis, J. E. 1997, in ASP Conf. Ser. 125, Astronomical Data Analysis Software and Systems VI, ed. G. Hunt & H. Payne (San Francisco: ASP), 477